

## Letters to *Analytical Chemistry*

# Transcutaneous Glucose Sensing by Surface-Enhanced Spatially Offset Raman Spectroscopy in a Rat Model

Jonathan M. Yuen,<sup>†</sup> Nilam C. Shah,<sup>‡</sup> Joseph T. Walsh, Jr.,<sup>†</sup> Matthew R. Glucksberg,<sup>†</sup> and Richard P. Van Duyne<sup>\*‡</sup>

Department of Biomedical Engineering and Chemistry Department, Northwestern University, 2145 Sheridan Road, Evanston, Illinois 60208

This letter presents the first quantitative, *in vivo*, transcutaneous glucose measurements using surface enhanced Raman spectroscopy (SERS). Silver film over nanosphere (AgFON) surfaces were functionalized with a mixed self-assembled monolayer (SAM) and implanted subcutaneously in a Sprague–Dawley rat. The glucose concentration was monitored in the interstitial fluid. SER spectra were collected from the sensor chip through the skin using spatially offset Raman spectroscopy (SORS). The combination of SERS and SORS is a powerful new approach to the challenging problem of *in vivo* metabolite and drug sensing.

The field of surface enhanced Raman spectroscopy (SERS) research has undergone a renaissance in the past decade, especially in the area of biological applications, due to the great advances made in the fabrication of large area, reproducible, long-lived SERS substrates.<sup>1</sup> Biological applications of SERS ranging from cancer detection<sup>2,3</sup> to the study of basic cell processes<sup>4,5</sup> have been vigorously pursued. However, most of this work has been carried out *in vitro*, due to the challenges posed by the complexity of the *in vivo* environment. These include (1) placement of the SERS-active surface *in vivo*; (2) the numerous interfering agents that can potentially adsorb to the SERS-active surface rendering it unresponsive to glucose or other target analytes; and (3) the natural inflammation and foreign body response (FBR) that occurs.

The majority of *in vivo* SERS work has been qualitative in nature and has used SERS as an alternative to fluorescence labeling.<sup>6,7</sup> In contrast, we demonstrated that SERS can be used *in vivo* to directly and quantitatively detect biological targets. The example pursued in our laboratory was an implantable SERS glucose sensor.<sup>8–13</sup> The SERS sensor utilizes the ability of Raman spectroscopy to specifically detect glucose and mitigates the inherently low intensity of Raman scattering by using surface-enhancement to amplify the intensity by factors of 10<sup>6</sup>–10<sup>8</sup>. In previous *in vivo* studies, a dorsal skinfold chamber was implanted in a rat for optical access to the SERS sensor.<sup>8,12</sup> At that time, a windowed chamber was the only method available that allowed collection of the SER scattering signal. While an effective laboratory tool, a more elegant solution was needed to push the use of an implantable SERS sensor toward clinical use.

The approach chosen was to remove the window and directly collect SER scattering transcutaneously. However, introducing the skin into the optical detection system presents a new set of challenges. The large refractive index change between skin and air immediately produces intensity losses due to back reflections.<sup>14</sup> Within the skin layers, light is further attenuated due to multiple scattering and absorption events. For example, the lipids in cell walls scatter light and blood absorbs light in the 400–700 nm region. Similarly, the protein keratin and the pigment melanin can

\* To whom correspondence should be addressed. E-mail: vanduyne@northwestern.edu.

<sup>†</sup> Department of Biomedical Engineering.

<sup>‡</sup> Chemistry Department.

- (1) Willets, K. A.; Van Duyne, R. P. *Annu. Rev. Phys. Chem.* **2007**, *58*, 267–297.
- (2) Boisselier, E.; Astruc, D. *Chem. Soc. Rev.* **2009**, *38*, 1759–1782.
- (3) Feng, S. Y.; Lin, J. Q.; Cheng, M.; Li, Y. Z.; Chen, G. N.; Huang, Z. F.; Yu, Y.; Chen, R.; Zeng, H. S. *Appl. Spectrosc.* **2009**, *63*, 1089–1094.
- (4) Huang, W. E.; Li, M. Q.; Jarvis, R. M.; Goodacre, R.; Banwart, S. A. In *Advances in Applied Microbiology*, Vol. 70; Elsevier Academic Press Inc.: San Diego, CA, 2010; pp 153–186.
- (5) Kneipp, J.; Kneipp, H.; Wittig, B.; Kneipp, K. *Nanomed.: Nanotechnol. Biol. Med.* **2010**, *6*, 214–226.

- (6) Qian, X. M.; Peng, X. H.; Ansari, D. O.; Yin-Goen, Q.; Chen, G. Z.; Shin, D. M.; Yang, L.; Young, A. N.; Wang, M. D.; Nie, S. M. *Nat. Biotechnol.* **2008**, *26*, 83–90.
- (7) Zavaleta, C. L.; Smith, B. R.; Walton, I.; Doering, W.; Davis, G.; Shojaei, B.; Natan, M. J.; Gambhir, S. S. *Proc. Natl. Acad. Sci. U.S.A.* **2009**, *106*, 13511–13516.
- (8) Lyandres, O.; Yuen, J. M.; Shah, N. C.; Van Duyne, R. P.; Walsh, J. T.; Glucksberg, M. R. *Diabetes Technol. Ther.* **2008**, *10*, 257–265.
- (9) Shafer-Peltier, K. E.; Haynes, C. L.; Glucksberg, M. R.; Van Duyne, R. P. *J. Am. Chem. Soc.* **2003**, *125*, 588–593.
- (10) Shah, N. C.; Lyandres, O.; Yonzon, C. R.; Walsh, J. T.; Glucksberg, M. R.; Van Duyne, R. P. *Anal. Chem.* **2005**, *77*, 6134–6139.
- (11) Stuart, D. A.; Yonzon, C. R.; Zhang, X.; Lyandres, O.; Shah, N. C.; Glucksberg, M. R.; Walsh, J. T.; Van Duyne, R. P. *Anal. Chem.* **2005**, *77*, 4013–4019.
- (12) Stuart, D. A.; Yuen, J. M.; Lyandres, N. S. O.; Yonzon, C. R.; Glucksberg, M. R.; Walsh, J. T.; Van Duyne, R. P. *Anal. Chem.* **2006**, *78*, 7211–7215.
- (13) Yonzon, C. R.; Haynes, C. L.; Zhang, X. Y.; Walsh, J. T.; Van Duyne, R. P. *Anal. Chem.* **2004**, *76*, 78–85.
- (14) Anderson, R. R.; Parrish, J. A. *J. Invest. Dermatol.* **1981**, *77*, 13–19.

both scatter and absorb light.<sup>15,16</sup> These difficulties are further compounded when illuminating and collecting from a subcutaneous sample since both the input laser excitation light must pass through the skin and the output Raman scattered light must pass back out through the skin to reach the detector. To address these problems, the approach chosen was spatially offset Raman spectroscopy (SORS).<sup>17</sup>

In SORS, Raman scattered light is collected from regions offset from the point of laser excitation at the sample.<sup>17</sup> In contrast, for normal Raman spectroscopy the excitation and collection points are coincident so that the surface of the sample gives the greatest contribution to the Raman spectrum. When spectra are collected some distance away from the excitation point, spectral features originating from underlying layers give a greater contribution than the surface.<sup>18,19</sup> Combining the sensitivity of SERS with the depth resolution of SORS yields a powerful new tool for biomedical sensing. During the time this research was conducted, Stone et al. independently combined SERS and SORS (SESORS) to capture *in vitro* spectra of NIR dye-tagged silver nanoparticles injected into pork tissue.<sup>20</sup> The conjugated dye was chosen to give a large signal when using near-infrared (NIR) excitation. This allowed for straightforward measurement of the tagged particles and determination of a detection threshold for particle density. The SESORS experiments reported here significantly extend the initial report<sup>20</sup> by demonstrating the acquisition of transcutaneous spectra *in vivo* and demonstrate an initial attempt at quantitative glucose detection.

## EXPERIMENTAL SECTION

**Materials.** All the chemicals were reagent grade or better and used as purchased. Silver pellets (99.99%) were purchased from the Kurt J. Lesker Co. (Clairton, PA). Titanium was obtained from McMaster-Carr (Chicago, IL) and cut into 0.5 mm thick, 8 mm-diameter disks. H<sub>2</sub>SO<sub>4</sub> (17.8 M) was purchased from EMD chemicals, NH<sub>4</sub>OH (28–30% in H<sub>2</sub>O), H<sub>2</sub>O<sub>2</sub> (30% in H<sub>2</sub>O), and ethanol were purchased from Fisher Scientific (Fairlawn, VA). Silica nanosphere solution (600 nm ± 10–15% diameter, 10.2% solid) was purchased from Bangs Laboratories, Inc. (Fishers, IN). Only Ultrapure water (18.2 MΩ cm<sup>-1</sup>) from a Millipore system (Marlborough, MA) was used. Glucose, decanethiol (DT), and 6-mercapto-1-hexanol (MH) were purchased from Sigma-Aldrich (St. Louis, MO).

**AgFON Fabrication and Incubation Procedure.** The titanium substrates were soaked in 6:1 H<sub>2</sub>O/H<sub>2</sub>SO<sub>4</sub> for 2 min, rinsed, and sonicated in a 5:1:1 H<sub>2</sub>O/30% H<sub>2</sub>O<sub>2</sub>/NH<sub>4</sub>OH solution for 10 min. Approximately 10 μL of nanosphere solution was drop-coated onto clean titanium substrates and allowed to dry under ambient conditions. Ag films (200 nm thick) were deposited over the nanosphere layer using a home-built thermal deposi-

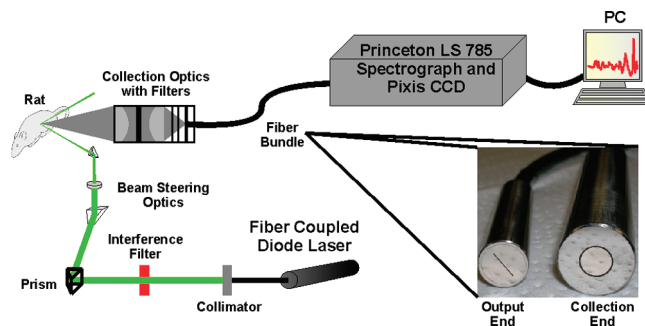


**Figure 1.** Schematic diagram of the SESORS apparatus. The inset shows the annular fiber bundle used to achieve offset collection.

tion system to form silver film over nanosphere (AgFON) substrates. The substrates were incubated in 1 mM DT in ethanol for 45 min and transferred to 1 mM MH in ethanol for at least 12 h to form a mixed DT/MH SAM. The AgFONs were kept in the 1 mM MH solution until used.

**Instrumentation.** The SORS system (Figure 1) was adapted from that described by Matousek.<sup>21</sup> A fiber coupled diode laser ( $\lambda_{\text{ex}} = 785 \text{ nm}$ ,  $P = 60 \text{ mW}$ , Newport Corp., Irvine, CA) was used as the illumination source, and an interference filter (Semrock, Rochester, NY) isolated the laser line. Optical quality prisms and mirrors (Thor Laboratories, Newton, NJ) were used to guide the laser to the sample. Identical lenses ( $D = 50.8 \text{ mm}$ ,  $f = 60.0 \text{ mm}$ , Thor Laboratories) were used to collect the scattered light and focus it into the fiber bundle. Between the lenses, a notch filter (Semrock, Rochester, NY) was used to reject the Rayleigh scattered light. Between the second focusing lens and the fiber bundle, another notch filter and long pass filter (Semrock, Rochester, NY) were used to further exclude the elastically scattered light.

The fiber bundle was a custom-made bundle (C-Technologies, Bridgewater, NJ) consisting of 26 fibers arranged in a 6 mm diameter circle at the collection head and aligned vertically at the detection end (Figure 1 inset). The Raman spectrometer was an Acton LS785 spectrograph paired with a Pixis 400BR CCD camera (Princeton Instruments, Trenton, NJ). Replacing the custom fiber bundle with a standard fiber bundle allowed the SORS system to function as a conventional Raman spectroscopy system.

**In Vivo Transcutaneous SESORS.** All surgical procedures followed protocols filed with the Northwestern University IACUC. A male Sprague–Dawley rat (453 g) was anesthetized with isoflurane (1.5–3%) throughout the surgical procedure and the duration of the experiment. The animal was checked for pain reactions by toe-tug and blink tests. None were observed. After the anesthetic had taken effect, the side and belly of the animal were shaved and chemically depilated. An incision was made in the skin and a pocket was blunt dissected into the subcutaneous space. A single DT/MH AgFON was placed in the pocket and the incision was closed with surgical clips. The rat was placed in the SORS apparatus and SESOR spectra were acquired. Excitation wavelength ( $\lambda_{\text{ex}}$ ) was 785 nm; excitation power ( $P_{\text{ex}}$ ) was 50 mW, and acquisition time ( $t_{\text{acq}}$ ) was 20 s.

**In Vivo Transcutaneous SESORS Glucose Measurements.** Experiments were conducted to gauge the viability of transcutaneous SESORS as a data collection technique for glucose measurements. A male rat (427 g) was anesthetized as previously

- (15) Bashkatov, A. N.; Genina, E. A.; Kochubey, V. I.; Tuchin, V. V. *J. Phys. D: Appl. Phys.* **2005**, *38*, 2543–2555.
- (16) Nielsen, K.; Zhao, L. S. J.; Stamnes, K.; Moam, J. In *Solar Radiation and Human Health*; Bjertness, E., Ed.; The Norwegian Academy of Science and Letters: Oslo, Norway, 2008.
- (17) Matousek, P.; Clark, I. P.; Draper, E. R. C.; Morris, M. D.; Goodship, A. E.; Everall, N.; Towrie, M.; Finney, W. F.; Parker, A. W. *Appl. Spectrosc.* **2005**, *59*, 393–400.
- (18) Matousek, P. *Chem. Soc. Rev.* **2007**, *36*, 1292–1304.
- (19) Matousek, P.; Stone, N. *Analyst* **2009**, *134*, 1058–1066.
- (20) Stone, N.; Faulds, K.; Graham, D.; Matousek, P. *Anal. Chem.* **2010**, *82*, 3969–3973.

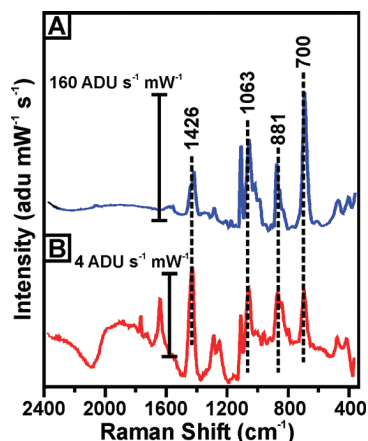


**Figure 2.** Comparison of (A) normal SER spectra and (B) *in vivo* transcutaneous SESOR spectra of a DT/MH-functionalized AgFON.  $\lambda_{\text{ex}} = 785 \text{ nm}$ ,  $P_{\text{ex}} = 50 \text{ mW}$ ,  $t_{\text{acq}} = 20 \text{ s}$ .

detailed and cannulated using PE 50 tubing for drug/glucose injections and blood glucose measurements, respectively. An AgFON sensor was implanted as described above; all incisions were shut with surgical clips, and the rat was placed in the SORS system. Following the experiment, the animals were sacrificed with an overdose of sodium pentobarbital (150 mg/kg) and bilateral thoracotomy. The glucose concentration in the rat was increased through intermittent intravenous infusion (1 g/mL in sterile PBS) over the course of the experiment and decreased by IV insulin injection (0.5 mL of 2 U/mL). A droplet of blood was drawn from the rat, the glucose level was measured with the Ascensia Elite home blood glucometer, and corresponding SESORS measurements were taken ( $\lambda_{\text{ex}} = 785 \text{ nm}$ ,  $P_{\text{ex}} = 50 \text{ mW}$ ,  $t_{\text{acq}} = 2 \text{ min}$ ). To keep the osmotic pressure of the rat at normal physiological levels, a volume of BSA (0.8% in sterile saline) equal to the blood removed was injected following each blood glucose measurement. The data were collected and analyzed by the partial least-squares leave-one-out (PLS-LOO) method described in our previous papers.<sup>8,10–13,22,23</sup> The calculations were performed with MATLAB (MathWorks, Inc., Natick, MA) and PLS\_Toolbox (Eigenvector Research, Inc., Manson, WA).

## RESULTS AND DISCUSSION

**SESORS from SAM Functionalized AgFON Surfaces.** *In vivo* transcutaneous SESORS spectra of a DT/MH functionalized AgFON were compared with the corresponding spectra of the functionalized AgFON taken *ex vivo* with the spectrometer in standard mode. Figure 2A shows the SER spectrum of a DT/MH AgFON. Figure 2B shows the *in vivo* SESOR spectrum of an implanted DT/MH AgFON. Representative peaks can be seen at 1426, 1063, 881, and 700  $\text{cm}^{-1}$ . The maximum peak intensity was 160  $\text{ADU s}^{-1} \text{ mW}^{-1}$  in the standard SERS spectrum and 4  $\text{ADU s}^{-1} \text{ mW}^{-1}$  in the transcutaneous SORS spectrum. Thus, the SERS signal is attenuated by approximately 95% due to the

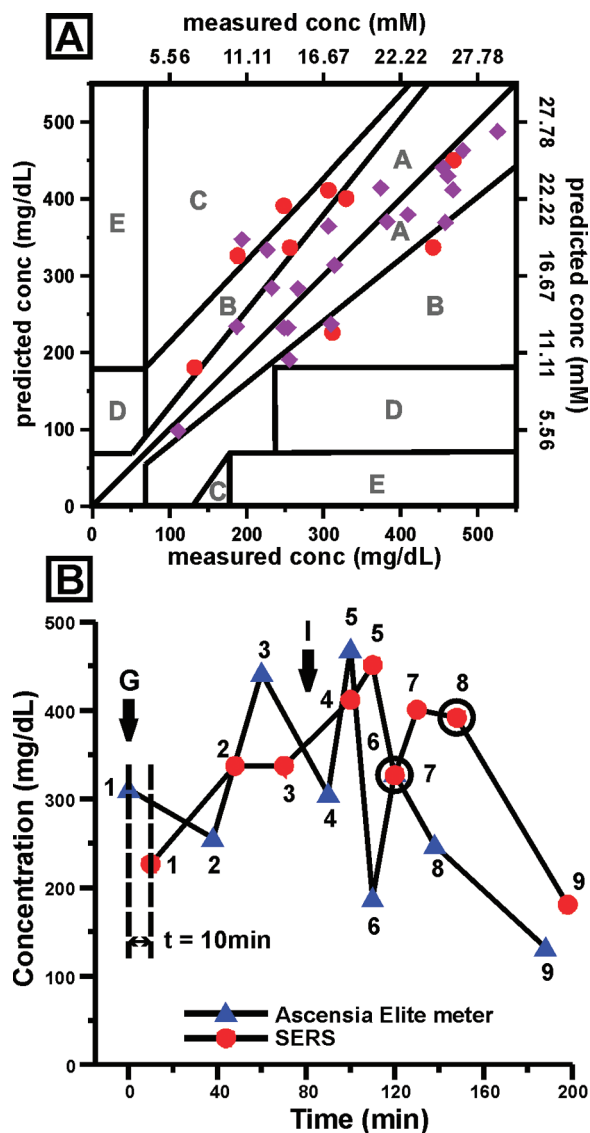


**Figure 3.** (A) Calibration (♦) and validation (●) sets of the first *in vivo* transcutaneous SESORS glucose measurements: 21 measurements were used for calibration, and 9 were for validation. RMSEC = 58.11 mg/dL (3.32 mM) and RMSEP = 96.35 mg/dL (5.35 mM). Mean absolute relative difference for calibration is 16.6% and for validation is 34.6%. (B) Timecourse of validation measurements. Glucose concentration is plotted with respect to time. The SERS measurements follow qualitative trends of the Ascensia Elite with the exception of the circled data points. SERS data point 6 and Ascensia meter point 7 overlap. Note glucose infusion (G) at 0 min and infusion of insulin (I) at 82 min.

presence of skin; however, all spectral features from the DT/MH AgFON remain easily observable with a high signal-to-noise ratio (S/N).

**Clarke Error Grid Analysis and Time Course Comparison.** The Clarke error grid was introduced over 20 years ago<sup>24</sup> and has become a common standard to compare the accuracy and performance of glucose sensors.<sup>25</sup> Predicted concentrations are plotted versus measured concentrations, and the graph is divided into five different zones. Measurements that fall in zone A are considered clinically accurate measurements, in zone B they lead

- (21) Matousek, P.; Draper, E. R. C.; Goodship, A. E.; Clark, I. P.; Ronayne, K. L.; Parker, A. W. *Appl. Spectrosc.* **2006**, *60*, 758–763.  
 (22) Beebe, K. R.; Pell, R. J.; Seasholtz, M. B. *Chemometrics: A Practical Guide*; Wiley Interscience: New York, 1998.  
 (23) Shah, N. C.; Lyandres, O.; Walsh, J. T.; Glucksberg, M. R.; Van Duyne, R. P. *Anal. Chem.* **2007**, *79*, 6927–6932.

- (24) Clarke, W. L.; Cox, D.; Gonder-Frederick, L. A.; Carter, W.; Pohl, S. L. *Diabetes Care* **1987**, *10*, 622–628.  
 (25) Clarke, W. L. *Diabetes Technol. Ther.* **2005**, *7*, 776–779.



to benign or no action by the patient, in zone C they lead to unnecessary action, in zone D they lead to a lack of action when glucose value correction is necessary, and, finally, in zone E they lead to actions that are opposite to those that are clinically necessary. Accurate sensing only results in data points within the A and B ranges of the grid.<sup>26</sup> Figure 3A shows a Clarke error grid analysis from *in vivo* transcutaneous SESORS glucose measurements. Unlike previous *in vivo* experiments, all measurements were not taken from a single position on the sensor, since using the annular fiber bundle to collect spectra inherently leads to a spatially averaged collection from a circular area instead of a single point. In addition, no holder was required to secure the sensor in position and the sensor was allowed to move with the body of the rat as it breathed. Thus, relative spatial motion between the sensor chip and the SORS probe was NOT problematic. In total, 30 measurements were taken. Twenty-one data points were correlated with the Ascensia Elite readings and used to create the calibration set. Nine measurements were used as independent data points for the validation set. A total of 7 of the 9 validation points fell within the A and B ranges, showing good predictive results. The mean absolute relative difference values for calibration was 16.6% and for validation 34.6%. Higher error (RMSEC = 58.11 mg/dL (3.23 mM) and RMSEP = 96.35 mg/dL (5.35 mM)) is seen than in previous *in vivo* results,<sup>8,12</sup> but given the added optical dispersion of the skin and the displacement of the sensor during the experiment this is not unexpected. It should be noted that these RMSEC values are similar to those reported in our earlier *in vitro* experiments.<sup>10</sup> The error can be improved by increasing the number of data points in the calibration.<sup>22</sup>

Figure 3B shows a comparison between readings of the Ascensia Elite and SESORS measurements as a function of time. Though not quantitatively identical, both effectively track the decrease of glucose concentration after dosing with insulin. The quantitative discrepancy between the sensors can be explained in part by their different sensing environments. The Ascensia Elite measures blood glucose concentration while the SERS sensor detects the concentration of glucose in the interstitial fluid. It is agreed that there is a delay associated with diffusion of glucose from blood vessels into the interstitial fluid, though estimates are inexact.<sup>27</sup> Therefore, it is unsurprising that the predicted values of the Ascensia Elite and the SERS sensor do not quantitatively agree. Points 6 and 8, which are circled, show a marked degree of deviation. A variety of sources of error can contribute to this deviation and will be investigated further in future experiments. Nevertheless, the extent of agreement is highly encouraging. In

addition to the different environments that the two sensors sample, the use of the Ascensia Elite as the calibration method for the SERS measurements also contributed to the differences observed. The scatter in the SERS measurements incorporates the error inherent in the Ascensia Elite, increasing the perceived SERS error. The current standard for accuracy of home blood glucose monitoring systems (ISO 15197) states that device measurements should fall within 20% of laboratory standard results 95% of the time (this corresponds to zone A in the Clarke error grid). This standard allows for large variations in glucose readings. Studies of commercial home glucose meters similar to the one used in our experiments have shown that most do not even meet this standard.<sup>26,28</sup> In a test of six home glucose meters, only one reached the ISO standard, with 96% of measurements falling within the A region. The least accurate meter showed only 67% of measurements falling within the A region. In addition to accuracy, home glucose meter precision was also measured. The precision varied from 5.5% to 8.4% (7.7–11.1 mg/dL).<sup>28</sup> Because of the calibrating method used in our study, the error in both the precision and the accuracy of the electrochemical sensing method contributed to even greater error in SERS measurements. Despite the numerical disparity, the results show that the SERS sensor is viable *in vivo* and can detect glucose concentration fluctuations over time.

## CONCLUSIONS

This work details the first proof-of-concept experiments for *in vivo* transcutaneous SER spectra taken using SORS. These results represent a significant step on the road toward an implantable, real time, continuous glucose sensor based on SERS. Current implanted amperometric sensors indirectly detect glucose through the flux of the molecule to the sensor surface.<sup>29–31</sup> Our SERS approach allows us to detect glucose directly, giving us the potential to exceed the capabilities of current implantable electrochemical glucose monitoring systems. We believe that further amplification of SERS signals by 100 times is possible with the next generation of substrates being developed in our laboratory.<sup>32</sup> The greater the SERS enhancement factor, the greater will be the accuracy of the SERS glucose sensor. Experiments are now in progress to test these new SERS substrates as well as new surface modification strategies designed to improve the reproducibility and longevity of the SERS sensor chip beyond levels currently demonstrated. Further, we are actively exploring modified surfaces with new partition/capture layers to expand the number of biological targets accessible to *in vivo* SERS. In light of these findings, it is now clear that skin is no longer an insurmountable barrier to quantitative *in vivo* SERS biosensing.

## ACKNOWLEDGMENT

This work was supported by NIH Grant 5R56DK078691-02, NSF Grant CHE-0911145, and AFOSR/DARPA Grant FA9550-08-1-0221.

Received for review July 23, 2010. Accepted September 8, 2010.

AC101951J

(26) Sheffield, C. A.; Kane, M. P.; Bakst, G.; Busch, R. S.; Abelseh, J. M.; Hamilton, R. A. *Diabetes Technol. Ther.* **2009**, *11*, 587–592.

(27) Wei, C.; Lunn, D. J.; Acerini, C. L.; Allen, J. M.; Larsen, A. M.; Wilinska, M. E.; Dunger, D. B.; Hovorka, R. *Diabetic Med.* **2010**, *27*, 117–122.

(28) Thomas, L. E.; Kane, M. P.; Bakst, G.; Busch, R. S.; Hamilton, R. A.; Abelseh, J. M. *Diabetes Technol. Ther.* **2008**, *10*, 102–110.

(29) Barone, P. W.; Parker, R. S.; Strano, M. S. *Anal. Chem.* **2005**, *77*, 7556–7562.

(30) Barone, P. W.; Strano, M. S. *J. Diabetes Sci. Technol.* **2009**, *3*, 242–252.

(31) Heller, A.; Feldman, B. *Chem. Rev.* **2008**, *108*, 2482–2505.

(32) Wustholz, K. L.; Henry, A.-I.; McMahon, J. M.; Freeman, R. G.; Valley, N.; Piotti, M. E.; Natan, M. J.; Schatz, G. C.; Van Duyne, R. P. *J. Am. Chem. Soc.* **2010**, *132*, 10903–10910.